SOLVING THE VIBRATION PROBLEM OF A VERTICAL MULTISTAGE CRYOGENIC PUMP

by

Ching M. Chang

Engineering Associate

and

Fred W. Braun

Manager

Union Carbide Corporation

Linde Division

Tonawanda, New York

Ching M. Chang is an Engineering Associate in the Research and Development Department of the Linde Division, Union Carbide Corporation, in Tonawanda, New York. One of his speciality areas is turbomachinery research and development.

He received a Ph.D. degree in Engineering from Technological University Aachen, Aachen, West Germany and a M.B.A. degree from State University of New York at Buffalo, in Buffalo, New York.

Dr.Chang is also an Adjunct Full Professor of Engineering at SUNY-Buffalo. He is a member of ASME and a registered professional engineer in the State of New York.

Fred W. Braun is Manager of Mechanical Equipment Engineering in the Gas Products Engineering Department of the Linde Division, Union Carbide Corporation, in Tonawanda, New York. He is responsible for specifying and troubleshooting mechanical equipment used by the Division.

Mr. Braun received his B.S. degree from the State University of New York at Buffalo, in Buffalo, New York. He is a member of ASME and a registered professional engineer in the State of New York.

ABSTRACT

Recent experience in solving the shaft breakage and seal rub problem of a vertical, eight-stage liquid nitrogen pump at a plant site is documented. Several initial field tests conducted to diagnose the vibration problem are described in detail. The pump is modelled as a dual level rotor bearing system, to account for the vibration characteristics of the support structure and pump casing bundle. A subsynchronous mode associated with the cantilever bending of the pump casing bundle was correctly predicted by this dual level analytical model. This subsynchronous mode would remain undetectable, if the pump were modelled as a single level system with rigid pump casing bundle and inflexible support structure. Also included in the analysis are pertinent representations for throttle bushings, wear rings, bearing bushings, and stator-impeller forces, based on empirical models selected from the open literature. The pump model was calibrated with vibration data of the support structure and the pump shaft. A comprehensive parametric study produced four cost-effective solutions, one of which was chosen for implementation. Subsequent field tests confirmed the reduction of shaft vibrations predicted by the analysis. The pump continues to operate satisfactorily.

The combined experimental and analytical approach outlined should be of interest to engineers responsible for solving the vibration problems of vertical multistage pumps.

INTRODUCTION

A combined experimental and analytical approach which led to the successful resolution of the severe vibration problem of a vertical multistage cryogenic pump at a plant site is described.

The pump design and a number of initial field tests conducted to assess the pump's vibration problem are presented as background in this case history. The subsequent section is devoted to the description of an analysis in which the pump is modelled as a dual level rotor bearing system. The models for wear rings and stator-impeller forces are discussed. The literature on fluid impeller interactions is briefly reviewed. The analytical model is calibrated against selected vibration measurements.

A large number of design factors have been varied to develop a set of cost-effective design modifications. The implementation of one of these design solutions produced a reduction of shaft vibration, which is sufficient to resolve the pump's vibration problem. Subsequent field tests validated the magnitude of the predicted vibration reduction.

Conclusions are presented, including an assessment of the general applicability of the outlined approach to solve vibration problems of vertical multistage pumps.

BACKGROUND

The subject pump is used to pump liquid nitrogen at 88.6 K ($-300°F$) under typical conditions. The pump operates at a flow rate of 27.13 liter/s (430 gpm) and a discharge pressure of 3.90 Mpa (565 psia). The unit is an eight-stage vertical turbine design with a direct mounted 200 hp, 3600 cpm motor. The impellers have a specific speed of 1450. A buffered labyrinth gas seal is employed to prevent liquid from leaking out the pump shaft. The pump is constructed of appropriate stainless steel, Monel and bronze alloys suitable for cryogenic temperatures.

The pump and the electric motor is depicted in Figure 1. The pump assembly is attached to a reinforced insulation box by a 0.045 m (1.75 in) thick mounting plate. The motor is installed onto the plate by a motor pedestal 0.533 m (21.0 in) in length. The motor pedestal is open on two sides to permit access to a rigid coupling that connects the motor and pump shaft. The coupling consists of the motor-half, spacer, and the pump-half parts. The labyrinth gas seal is secured on the top side of the mounting plate directly beneath the motor

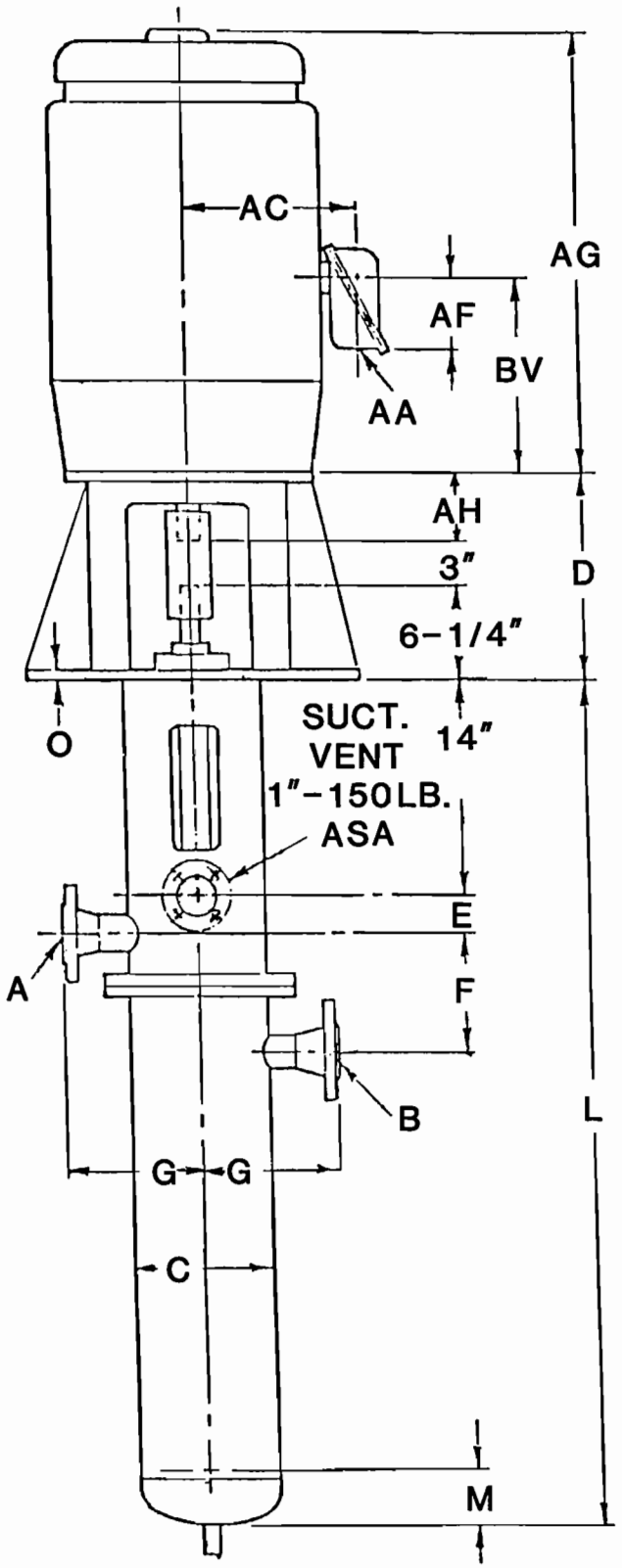

Figure 1. Vertical Multistage Cryogenic Pump.

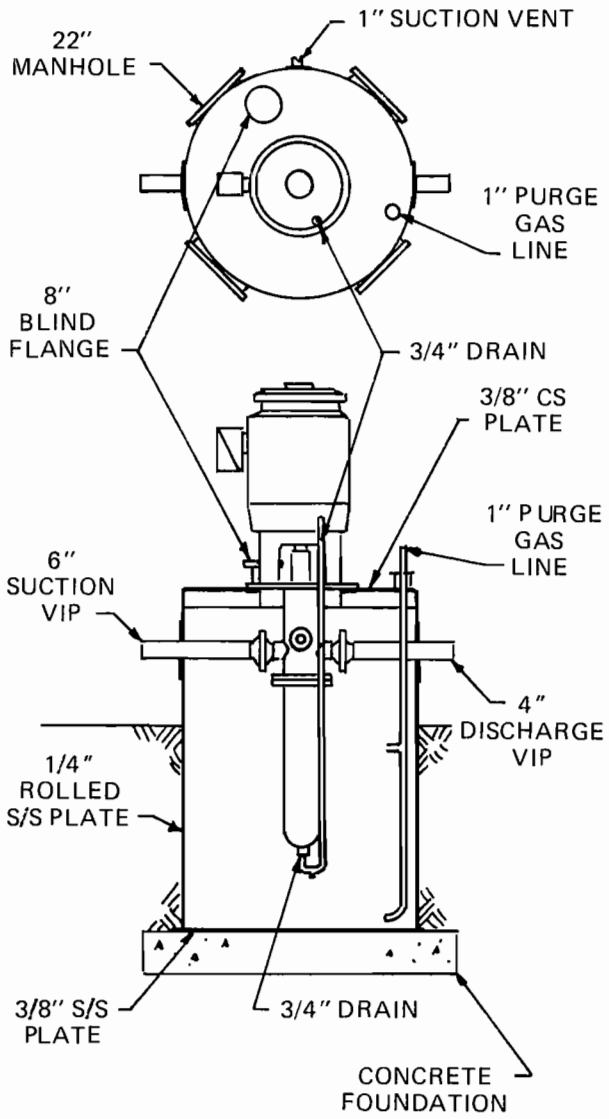

Figure 2. Cryogenic Pump Cold Box Design.

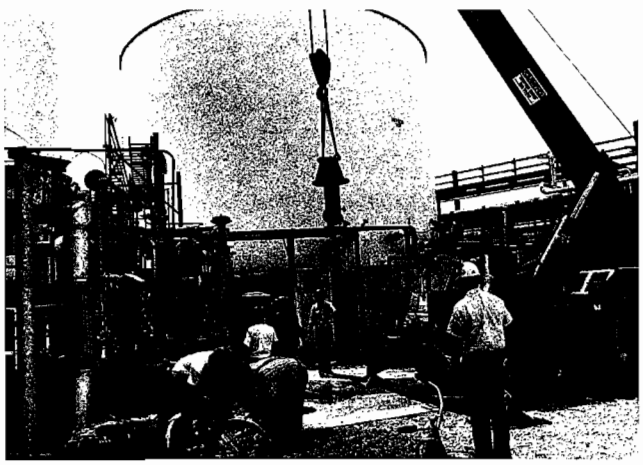

Figure 3. Installation of the Pump.

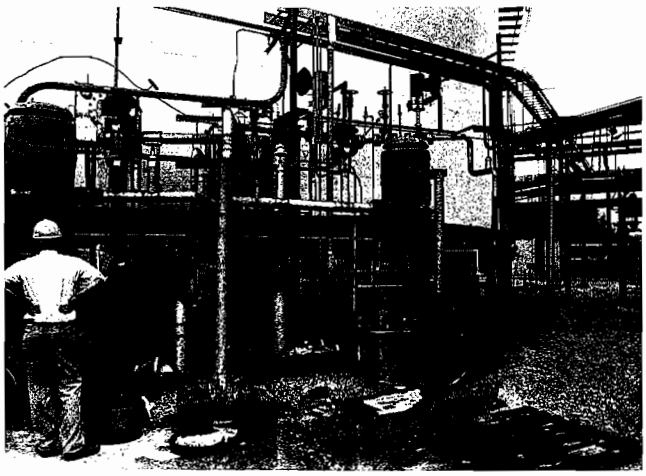

Figure 4. Pump Installed in Place.

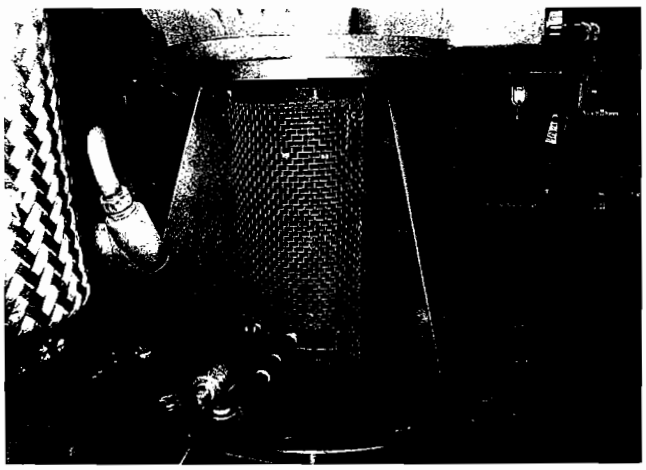

Figure 5. Motor Pedestal.

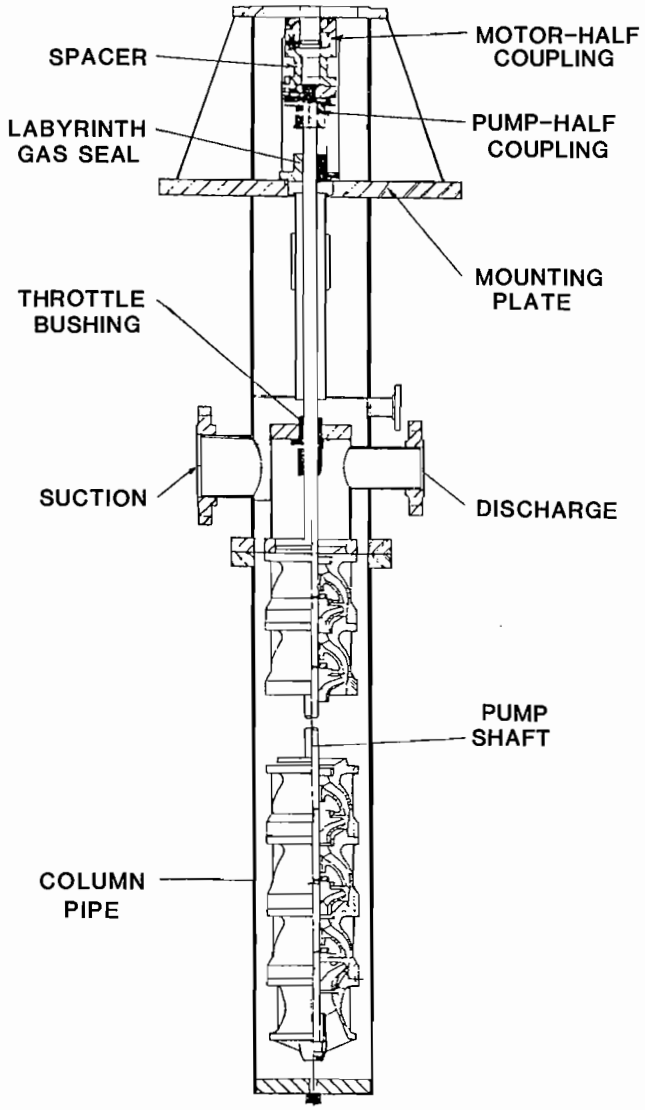

Figure 6. Pump Cross-Section.

coupling. The cryogenic pump cold box is shown in Figure 2. The pump assembly and its installation is depicted in Figures 3 and 4. A view of the motor pedestal is presented in Figure 5.

The upper motor bearing is a combined radial and thrust anti-friction bearing, whereas, the lower motor bearing is a radial rolling element ball bearing. Stiffness coefficients for these motor bearings were available from the vendor.

The pump is located entirely below the mounting plate. A column pipe serves as the pump inlet manifold, with the first stage being at the bottom most position. The discharge of the first stage is directed by internal passages to the suction of the second stage. The liquid is pumped upwards in this manner. The section view of the pump-motor assembly is presented in Figure 6. A throttle bushing separates the pump discharge from the pump suction, and is exposed a pressure difference of 3.743 Mpa (543 psia) there between.

Graphite bronze bearing bushings are placed between stages and at the inlet of the first stage. All bearing bushings are lubricated by liquid nitrogen under a stage differential pressure. Nitrogen leakage between stages is controlled by small clearances at the impeller and casing wear rings. The detailed arrangement of the pump stages is depicted in Figure 7.

The largest unsupported span between the lower motor bearing and the throttle bushing is 1.32 m (52 in). The span between the throttle bushing and the stage number 8 bearing bushing is 0.376 m (14.8 in).

The impellers are spaced at 0.1921 m (7.5625 in) intervals. They are secured to the pump shaft by keys, snap rings and fasteners in the axial direction. The process of installing impellers at room temperature is shown in Figure 8. Under cryogenic operating conditions, the impeller shrinks onto the shaft. The pump assembly cannot be mass balanced at room temperature, due to the long and very flexible shaft, along with an impeller-to-shaft clearance fit of 0.089 mm (3 to 4 mils). The individual impellers are shop balanced to below 36.00 gm-mm (0.05 oz-in). The shaft diameter is 0.0365 m (1.436 in).

Initially, the pump was installed and commissioned without much difficulty. A significant calendar time elapsed, before the pump was restarted in 1984. After approximately 25 hours of operation, the pump shaft failed at the upper (eighth stage) snap ring position. The failure surface was badly smeared. While no positive identification of the failure mode could be made, it was hypothesized that the failure was likely due to bending or torsional fatigue rather than overload. No damage was made to the bearings or throttle bushing; however, the labyrinth gas seal showed some signs of contact.

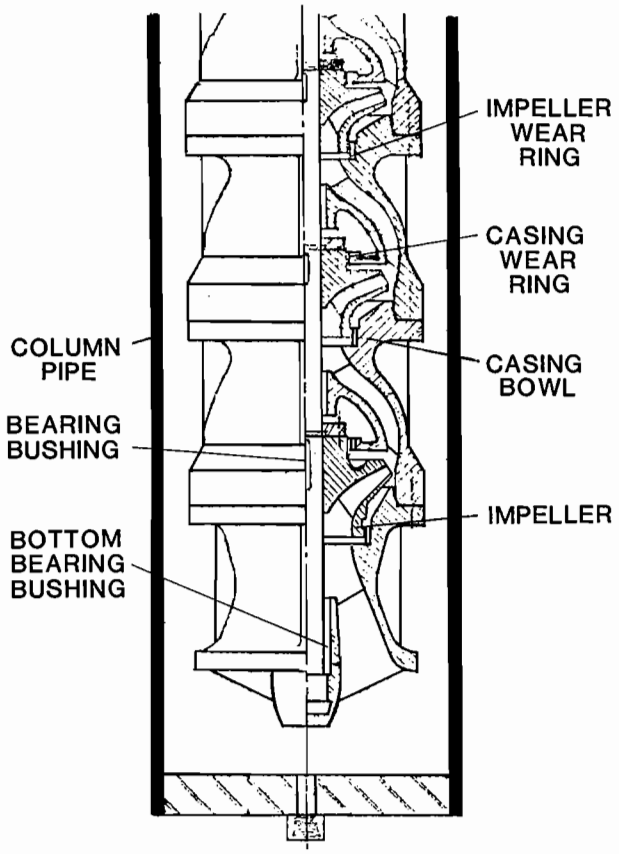

Figure 7. Enlarged View of Pump Stages.

The unit was rebuilt using a new shaft with new bearing bushings of known clearance, and a new labyrinth gas seal. The unit was returned to service. On initial startup, the pump shaft wiped the labyrinth gas seal. Velocity and acceleration transducers were placed on the motor pedestal and mounting plate in an attempt to understand the pump's vibrational modes and frequencies. No instrumentation was placed on the pump end, since it was inaccessible within the insulation box. Results indicated that the mounting plate was nearly stationary, while the motor's vibration orbit was highly elliptical. The major axis of the elliptical path coincided with the weak axis of the motor pedestal. The major vibration frequency coincided with motor speed.

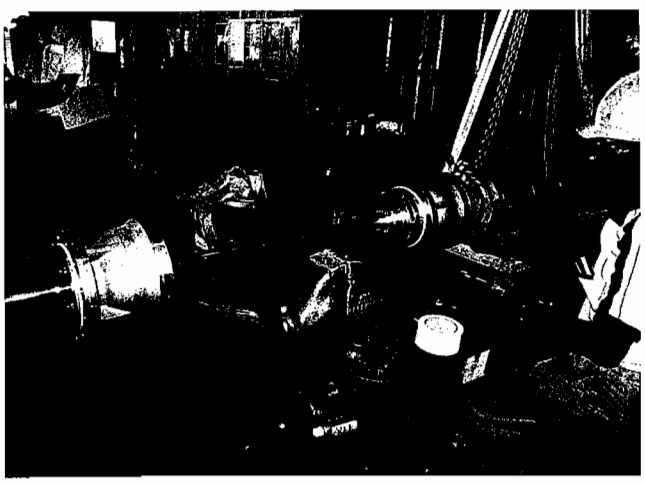

Figure 8. Installation of Pump Impellers.

The motor pedestal was then reworked to make the stiffness more or less uniform in all directions. The motor was rebalanced and the reworked unit was reinstalled.

Additional non-contacting eddy current proximity probes were installed to monitor the relative motion of the shaft with respect to motor pedestal. The probes were located 0.0127 m (0.5 in) above the labyrinth gas seal, and placed 90 degrees to each other. They were oriented to coincide with the major and minor axes of the motor orbit. A keyphasor was also installed to monitor the phase angle.

A calibrated hammer was fabricated that could apply a known force of random frequency content to the pump support structure. The motor was impact tested numerous times at different positions and the vibrational response was captured for further evaluation. No frequency response was found that could have been excited by the motor running speed or a multiple of it.

Upon restart, normal operating conditions were achieved. It was found that the vibration amplitude of the motor was reduced significantly and the orbit was now more nearly circular. However, the shaft vibration remained excessively high near the labyrinth gas seal and the shaft contacted the seal at one point. As shown in Figure 9, the shaft vibration was in excess of 0.193 mm (7.60 mils) peak-to-peak.

The unit was restarted, brought up to full speed normal operation condition and shut down for several times. All data were recorded on magnetic tapes for subsequent data reduction and evaluation. It became rather apparent that there was a serious rotordynamic problem within the pump assembly. It was decided to perform a rotordynamic analysis and, at the same time, disassemble the pump for inspection.

The motor and impellers were rebalanced to a tighter tolerance. All critical dimensions that could affect alignment were reworked to ensure that the assembly would be properly aligned when reassembled. The rigid coupling was also reworked to a tighter tolerance both on alignment and balance. Reassembly awaited results of the rotordynamic analysis.

A maximum peak-to-peak shaft vibration of 0.076 mm (3.0 mils) in the labyrinth gas seal location was selected as a reasonable goal to be achieved by modifying the pump design. Pump modification proposals are to be developed based on this rotordynamic analysis. Preference is given to

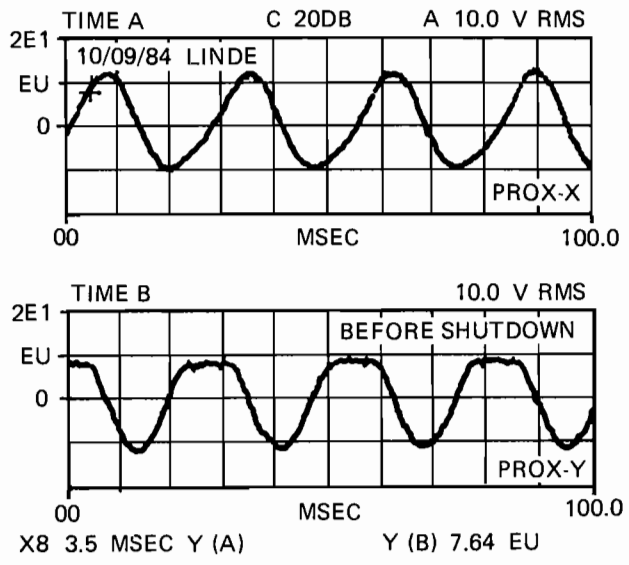

Figure 9. Vibration Signals Indicating Seal Rub.

design solutions which require the least amount of changes to the pump assembly, while providing an adequate reduction of the shaft vibration.

ANALYSIS

The vertical pump is characterized by a very long flexible shaft with a large number of rotating stages, a pump impeller bundle which is free-hanging inside of another free hanging column pipe, and a heavy motor which sits on top, driving the pump shaft. This design calls for a rotordynamic analysis which considers the vibrations of the motor pedestal above ground and the pump casing bundle below ground.

Preliminary undamped critical speed analyses showed that a subsynchronous mode could not be detected by the analysis, if the pump were modelled as a single level system, assuming both the support structure and pump casing bundle being maintained rigidly in space. The resulting mode shape computation confirmed that this subsynchronous mode is due to the cantilever bending of the pump casing bundle. A comprehensive stability analysis showed further that modelling the pump as a single level system resulted in overestimating the pump's stability margin.

The pump is thus modelled as a dual level rotor bearing system. Pertinent models for throttle bushings, wear rings, bearing bushings and stator impeller forces are incorporated into the analysis. Since the primary concern was the excessive shaft vibration at the labyrinth gas seal location, the emphasis of the analysis was placed on studying the pump's forced response characteristics. Although the method of modelling a turbomachine as a dual level system is not new, its application to a vertical, multistage pump has probably not been attempted.

Gunter, et al. [1], performed stability analyses for a vertical 24-stage high pressure injection pump of double case construction. Various bearing designs were studied to improve the pump's stability margin during startup, when there were insufficient axial pressure drops across the seals and wear rings to stabilize the system. The pump was modelled as a single level rotor bearing system, without taking into account the support structure vibration. An adjustment was made, however, to the lower motor bearing stiffness to account for a flexible bearing retainer cartridge. The pump's impeller bundle is pivoted in a spigot fit connected to the outside casing. Operating conditions were shown to strongly affect the stiffness and damping characteristics of seals, wear rings and throttle bushings. No forced response analyses were carried out.

Gopalakrishnan et. al. [2, 3], also stressed the importance of modelling seals, wear rings and stator-impeller forces properly in defining the critical speeds of pumps. A differentiation is made between dry and wet critical speeds, which are related to the absence and presence, respectively, of the so-called Lomakin effect in wear rings, seals and/or bushings.

Bossman [4], published the test results of a vertical water pump and concluded that:

- Hydraulic effects in pumps appear to be several orders of magnitude higher than those due to imbalance and alignment.
- Enlargement of clearance causes the pump to become less stable and to exhibit higher vibrations.
- Only when located near the impellers can a proximity probe register the subsynchronous vibration of the pump.

His results supported the finding that it is important to properly model the wear rings, seals and bushings under pertinent operating conditions.

Flows in wear rings and bushings under axial pressure gradients have been the subject of many investigations in the literature, for example, Black [5], Childs [6], and Allaire, et al. [7], and Kim and Childs [8]. Important test data on stator-impeller forces were published by Jerry, et al. [9, 10], and Chamieh, et al. [11].

More recently, Gopalakrishnan [12], reviewed the data for wear rings, bushings and stator-impeller forces available in the literature. For a horizontal multistage feed pump, he found that the effect of wear rings on the pump's stability and critical speeds is much more significant than that due to stator-impeller forces. The wear ring effects tend to suppress critical speeds and postpone instability, whereas those of stator-impeller tend to lower the critical speeds as well as the instability onset speed. No results were presented for vertical pumps.

Many experimental methods were described in open literature to resolve vibration problems of specific pumps, such as Starr [13], Jones [14], Makay [15], Meyer [16], Sosa, et al. [17], Marenco, et al. [18], Goldman [19], Mondy, et al. [20], and Mondy [21], and Smith, et al. [22]. Most of these methods, while successfully applied to the pumps studied, are not generally applicable to pumps of different designs, particularly the vertical pump described herein.

ANALYTICAL MODEL

Unlike the pump studied by Gunter et al. [1], wherein its casing bundle is pivoted at a spigot fit of its outer casing, the casing bundle of this pump is unsupported at its lower end. Both the casing bundle and the cylindrical column pipe are free-hanging, as the entire motor pump unit is rigidly supported only at the mounting plate location (Figures 1 and 2). Because of this specific pump support design, it was elected to model the pump motor support structure as level-1 rotor and the rotating assembly as level-2 rotor in a dual level rotor bearing system model.

The imbalance of individual coupling pieces has been measured in the shop. The resulting imbalance of the assembled coupling, on the other hand, is difficult to estimate accurately. In this analysis, it is being treated as an unknown parameter, which has been systematically varied to calibrate the analytical model. The analytical model is regarded as properly calibrated, if the field measured vibrations at the following three stations are matched simultaneously by the model's predictions: the absolute support structure vibrations at the motor-top and motor-bottom stations, and the relative vibration of the shaft with respect to motor pedestal at the shaft probe location, 12.70 mm (0.5 in) above the labyrinth gas seal station.

The following additional measurements have been incorporated into the analytical model:

- Mass and support stiffness of the motor pedestal.
- Mass and imbalance of impellers and motor rotor.
- Diametral clearances in impeller wear ring, casing wear ring and bearing bushing of each pump stage measured at room temperatures, adjusted for expected shrinkage at the cryogenic operation temperatures. The shrinkage adjustment was made based on results of sample tests conducted in the laboratory.

A 49-station model was established for the motor pump unit, including 28 bearings consisting of two motor bearings, one throttle bushing, a set of impeller wear ring, casing wear ring, and bearing bushing for each of the eight impeller stages and the bottom bearing bushing.

The following models for smooth wear rings (also bushings) and stator-impeller forces are adopted from [12] for

use in this study. The smooth wear ring coefficients are functions of the pressure drop across the rings:

$$K_{xx} = K_{yy} = m_L \omega^2 \tag{1}$$

$$C_{xx} = C_{yy} = 2\, c\, \omega \tag{2}$$

$$K_{xy} = -K_{yx} = c\, \omega^2 \tag{3}$$

$$C_{xy} = C_{yx} = 0 \tag{4}$$

where

$$m_L = \frac{\pi}{4} D\, L \frac{\frac{\lambda L}{2(1+\xi_1)}}{[\frac{\lambda L}{2(1+\xi_1)} + H]^2} \Delta P\, \phi \frac{1}{\omega^2} \tag{5}$$

$$c = \frac{\pi}{8} \frac{D\, L^2}{H} \frac{[1+\xi_1 + \frac{\lambda L}{6H}]}{[1+\xi + \frac{\lambda L}{2H}]^{1/2}} [\frac{\rho\, \Delta P}{2\, g}]^{1/2} \phi \frac{1}{\omega} \tag{6}$$

with

$\xi = C_g/C^* =$ Damping coefficient/critical damping coefficient

ρ = Fluid density
ω = Speed of rotation
D = Shaft Diameter
L = Length of Wear Rings
ΔP = Pressure drop
g = Gravitational Constant
λ = Friction Factor
ξ_1 = Entrance loss coefficient
H = Radial clearance

The short circuit factor ϕ is defined as

$$\phi = \frac{1}{1+(L/D)^2}$$

...Equations 7-10 set — (GUIDE)...

$$K_{xx} = -m_h \omega^2 = K_{yy} \tag{7}$$

$$K_{xy} = m_h' \omega^2 = -K_{yx} \tag{8}$$

$$m_h = K^*_{xx} \pi \rho r_2^2 b_2 \tag{9}$$

$$m_h' = K^*_{xy} \pi \rho r_2^2 b_2 \tag{10}$$

where

K^*_{xx}, K^*_{xy} = Non-dimensional stiffness coefficients, dependent on stator-impeller geometry and flow factor.
r_2 = Impeller tip radius.
b_2 = Tip width at impeller exit

For a given geometry, this model indicates that the stiffness coefficients for the stator-impeller effects vary with the fluid density and speed only. Based on test data published by Chamieh et al. [11], the following values are selected for use in our model:

$$K^*_{xx} = 2.0$$

$$K^*_{xy} = 0.9 \tag{11}$$

The pertinent stiffness and damping coefficients for wear rings, throttle and bearing bushings and stator-impeller forces for the present pump are summarized in Table 1.

Table 1. Summary of Stiffness and Damping Coefficients.

D = Diameter, mm (inch)
L = Length, mm (inch)
H = Radial Clearance, mm (mil)
Phi = Short Circuit Factor (-)
Kxx = Kyy = Principal Stiffness, Newtons/m (lbf/inch)
Kxy = -Kyx = Cross-Coupling Stiffness, Newtons/m (lbf/inch)
Cxx = Cyy = Principal Damping Coefficient, Newtons.sec/m (lbf.sec/inch)
Cxy = Cyx = 0.00
ΔP = Pressure Drop, Mpa (Psia)

DESCRIPTION	D	L	H	Phi	Kxx	Kxy	Cxx	ΔP
IMPELLER WEAR RING (FIRST STAGE)	123.4 (4.86)	10.7 (0.42)	0.216 (8.50)	0.9925	2248 (1848)	831 (683)	4.40 (3.6)	0.28 (41)
IMPELLER WEAR RING (2 TO 8 STAGES)	98.8 (3.89)	15.1 (0.59)	0.216 (8.50)	0.9772	2600 (2136)	1290 (1061)	6.85 (5.6)	0.28 (41)
CASING WEAR RING (1 TO 8 STAGES)	91.7 (3.61)	13.5 (0.53)	0.216 (8.50)	0.9788	2143 (1762)	960 (789)	5.11 (4.2)	0.28 (41)
BOTTOM BEARING BUSHING	36.5 (1.44)	91.5 (3.60)	0.080 (3.13)	0.1370	11404 (9377)	30980 (25472)	128 (105)	0 (0)
BEARING BUSHING (2 TO 8 STAGES)	36.5 (1.44)	50.8 (2.00)	0.080 (3.13)	0.3400	1626 (1337)	8032 (6604)	42.6 (35)	0.40 (58)
THROTTLE BUSHING DESIGN	36.4 (1.44)	146 (5.74)	0.160 (6.25)	0.0589	2403 (1976)	18170 (14940)	96.1 (79)	3.20 (464)
STATOR-IMPELLER FORCES	184.2 (7.25)	21.0 (0.83) (=B2)	--	---	- 893 (- 734)	402 (331)	--	--

The stator-impeller forces, although assumed to act at the impeller's centroid, are modelled by distributing the pertinent stiffness coefficients to the impeller casing wear rings of the same stage, equally.

Since the major objective of setting up the analytical model is to properly predict the unbalance responses of the pump shaft, especially at the labyrinth gas seal (station number 13) where seal rub occurred, it is very essential that the model be calibrated using available test data. It is also important to assess the sensitivity of the model to some of the less certain design factors, such as the actual clearances of wear rings and bearing bushings. The decision was made to use the RESP2V3 program deveoped by the University of Virginia ROMAC Industrial Consortium [21]. For use in this study, the original version of this dual level response analysis program was extended to handle up to 30 bearings.

RESULTS

The baseline vibration characteristics of the pump, as predicted by the calibrated analytical model, are shown in Figure 10. Both the absolute vibration of the support structure and the relative vibration of the pump shaft are approximately illustrated by straight line segments. The

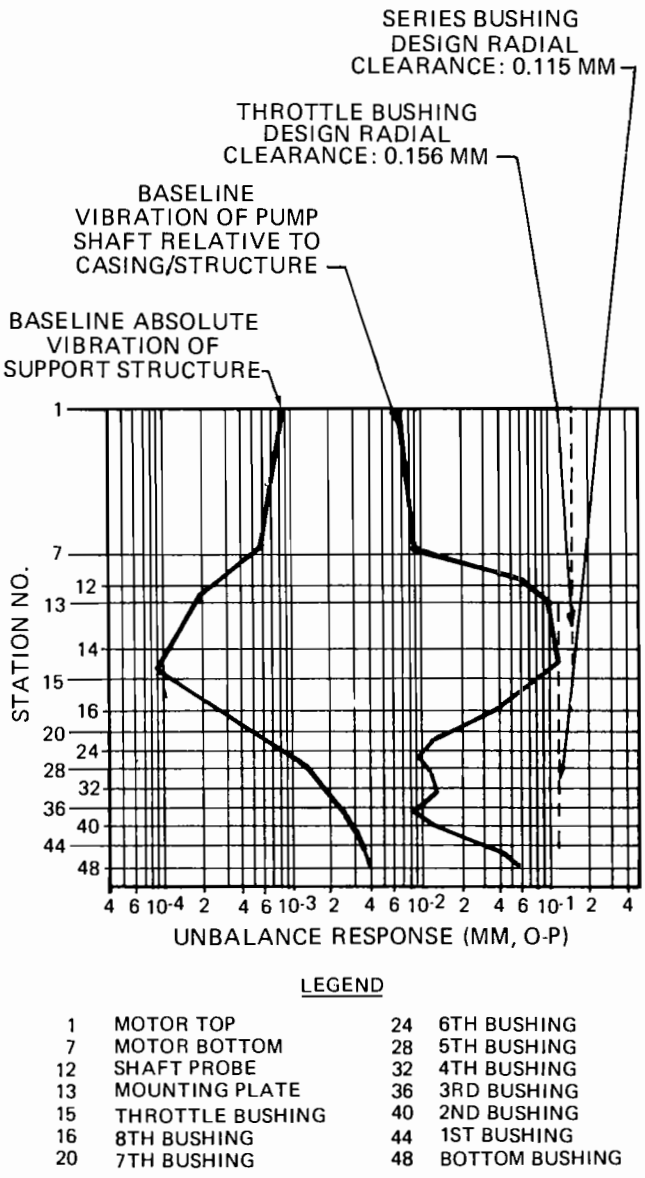

Figure 10. Base-Line Vibrations of the Pump.

absolute vibrations of the support structure at the motor top (station number 1) and motor-bottom (station number 7) locations and the relative vibration of the pump shaft with respect to the support structure at the shaft probe (station number 12) location are matched with test data.

A sensitivity analysis indicated that the shaft vibration at the labyrinth gas seal location (station number 13) changes insignificantly, if the following factors are varied in the ranges shown:

- Wear ring stiffness (± 20 percent)
- Stator-Impeller forces (± 100 percent)
- Series Bearing stiffness (± 50 percent).

Thus, observations have been that for modelling the unbalance response of the above-ground sections (stations 1 to 13) of vertical pumps of the type presented, very accurate representations of wear rings, bearing bushings and stator-impeller forces do not appear to be required.

Further studies indicate that the motor-bearing stiffness and impeller imbalance affect the shaft vibrations at station number 13 also only slightly.

A comprehensive parametric study followed which identified the following practical design modifications as effective in reducing the shaft vibrations at the labyrinth gas seal (station number 13) and throttle bushing (station number 15) locations:

- Reduce the coupling imbalance.
- Shorten the support-free shaft span between the lower motor bearing and the throttle bushing by:
  - relocating the present throttle bushing, or
  - adding another throttle bushing in between the two.
- Increase the throttle bushing stiffness.
- Reduce the bottom bearing bushing stiffness.

PROPOSED SOLUTIONS

Four specific solutions were developed to employ a combination of the aforementioned design modifications in order to attain the desired goal of vibration reduction at the labyrinth gas location (station number 13):

Proposed Solution 1 (Figure 11). Relocate the throttle bushing to a new station, number 14, which is about 0.211 m (8.3 in) above its current location (station number 15), and trim-balance the coupling to reduce its imbalance by 40 percent. This solution is expected to reduce the shaft vibration by

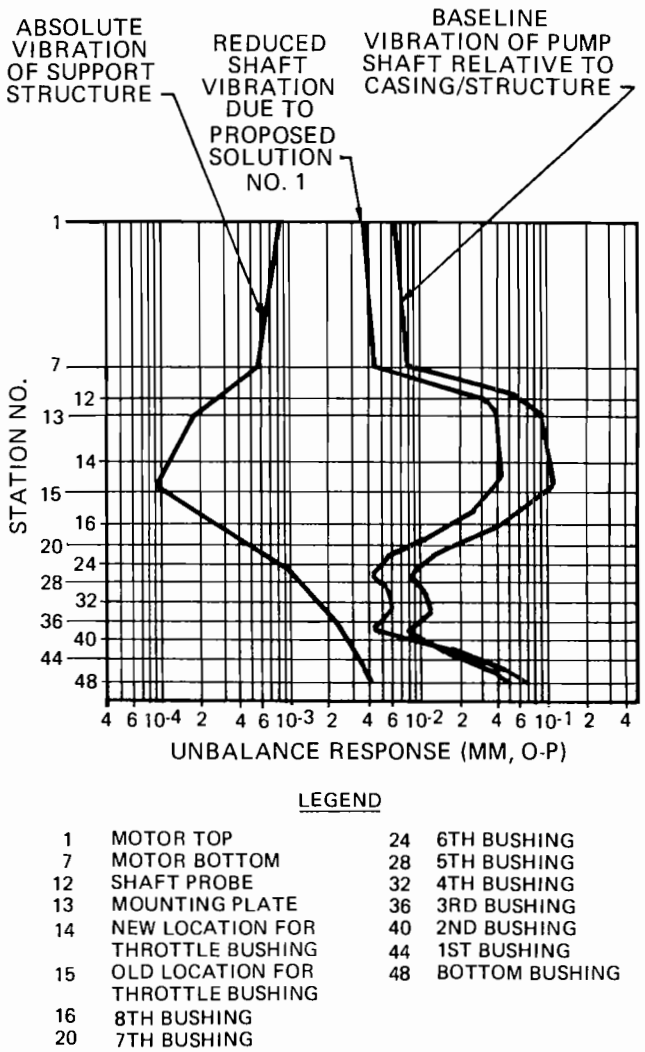

Figure 11. Proposed Solution 1.

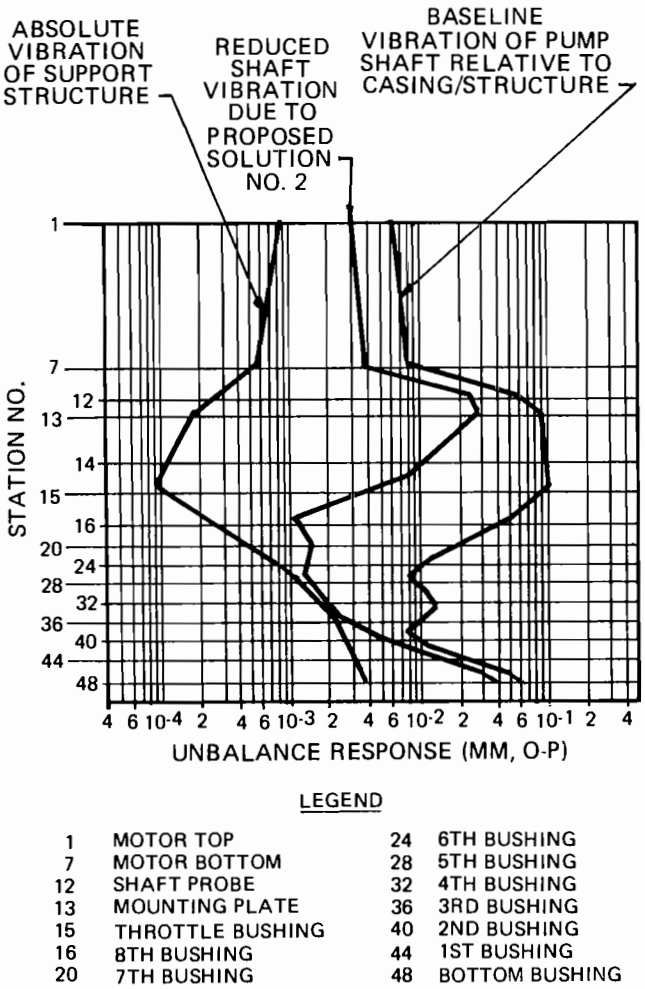

Figure 12. Proposed Solution 2.

55.3 percent, from 0.1930 mm (7.6 mils) to 0.0863 mm (3.4 mils) peak-to-peak, at station number 13.

Proposed Solution 2 (Figure 12). Increase the stiffness of the throttle bushing 10 times, reduce the coupling imbalance by 40 percent and decrease the bottom bearing stiffness by 90 percent. This solution is expected to reduce the shaft vibration by 65.8 percent, to 0.066 mm (2.6 mils) peak-to-peak, at station number 13.

Proposed Solution 3 (Figure 13). Add a second throttle bushing of equal stiffness to station number 14, and trim-balance the coupling to reduce its imbalance by 40 percent.

This solution is expected to reduce shaft vibration by 57.9 percent, to 0.0813 (3.2 mils) peak-to-peak, at station number 13.

Proposed Solution 4 (Figure 14). Reduce the motor pedestal stiffness to 1/100 of its present value, raise the throttle bushing stiffness 10 times, reduce the coupling imbalance by 40 percent, and reduce the stiffness of the bottom bearing bushing stiffness by 90 percent.

This solution is expected to reduce shaft vibration by 74.5 percent, to 0.0493 mm (1.94 mils) peak-to-peak, at station number 13.

All of these proposed solutions require that the coupling be trim balanced. Of the parameters studied, coupling imbalance is the single most important factor affecting the shaft vibration at station number 13. An increase of throttle bushing stiffness must be accompanied by a reduction of the bottom bearing bushing stiffness in order to prevent a buildup of excessive vibration at the lower pump end. The proposed Solution 2 has an advantage over Solution 1, because it is the simpler solution to implement.

Both Solutions 1 and 3 require that a throttle bushing be installed at the station number 14. Solution 3 produces a slightly larger expected benefit over Solution 1. The implementation of Solution 4 requires that a new motor pedestal be constructed rendering it somewhat impractical, although it would produce the largest reduction of shaft vibration among the solutions proposed.

CHOICE OF SOLUTION

Each of the proposed solutions has advantages and disadvantages. The easiness of implementation is of practical importance. In addition, it is also preferable to change one thing at a time to enhance the likelihood of achieving success in a timely manner. Also considered was the possibility that the throttle bushing stiffness would be reduced over time, due to wear. The proposed Solution 1 was thus adopted for field implementation.

FIELD TESTS

The shaft vibration at the probe location (station number 13), before and after the implementation of Solution 1, is illustrated in Figures 15 and 16, respectively. The vibration

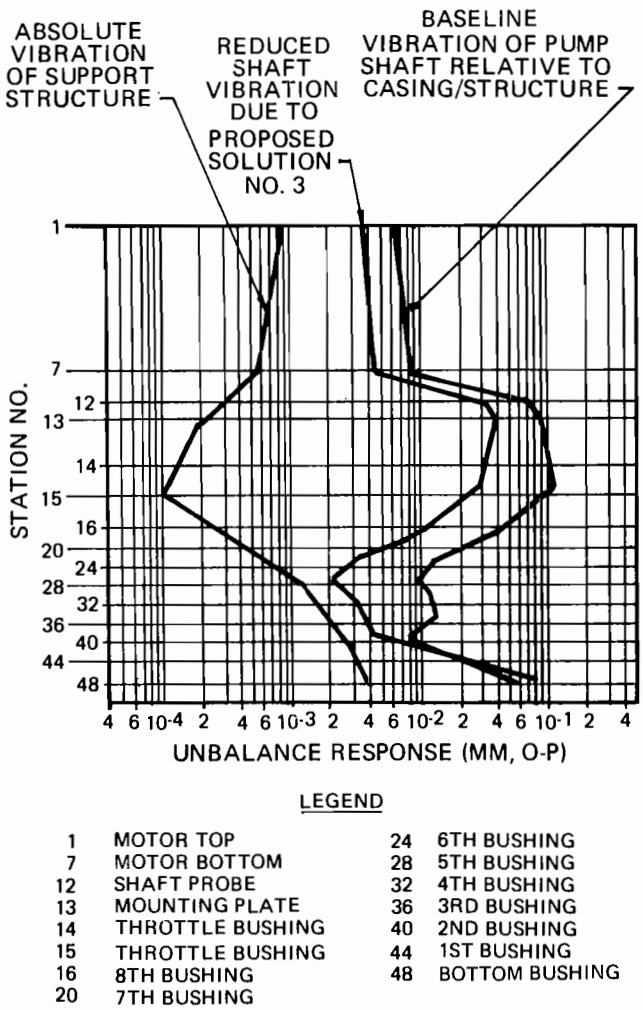

Figure 13. Proposed Solution 3.

data are compared in Table 2. Since the phase angle data were not recorded, the measured vibrations could not be properly compensated. Assuming that the vibrational signals are all in phase, the running speed shaft vibration is shown to have been reduced by 70.7 percent to 54.9 percent. The vibration level of the pump remained steady after a field

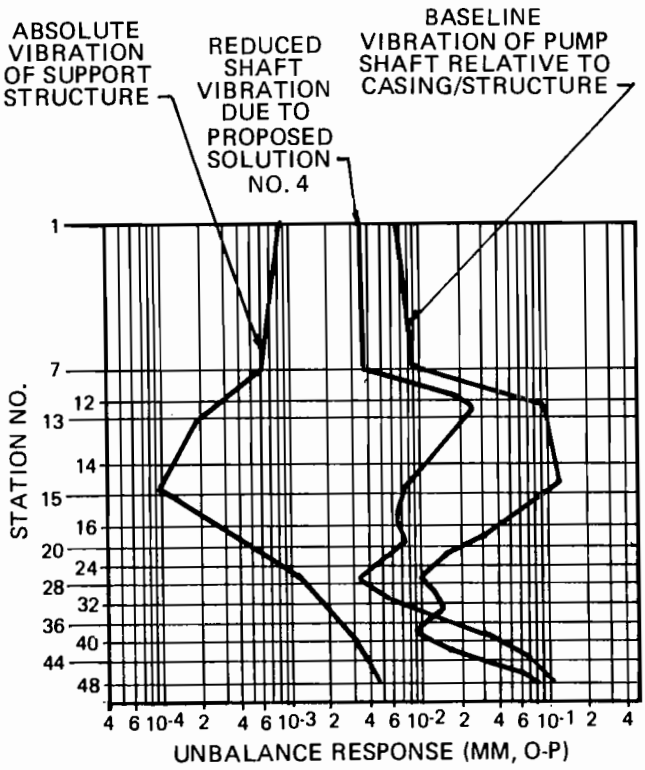

LEGEND

1	MOTOR TOP	24	6TH BUSHING
7	MOTOR BOTTOM	28	5TH BUSHING
12	SHAFT PROBE	32	4TH BUSHING
13	MOUNTING PLATE	36	3RD BUSHING
15	THROTTLE BUSHING	40	2ND BUSHING
16	8TH BUSHING	44	1ST BUSHING
20	7TH BUSHING	48	BOTTOM BUSHING

Figure 14. Proposed Solution 4.

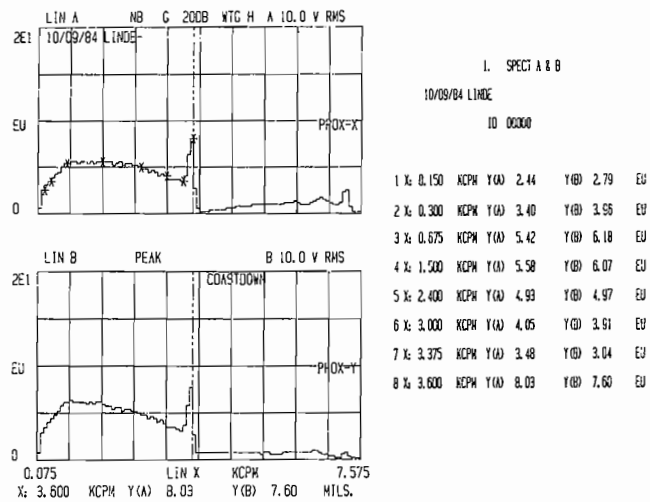

Figure 15. Pump Vibration Before Implementation of Solution 1.

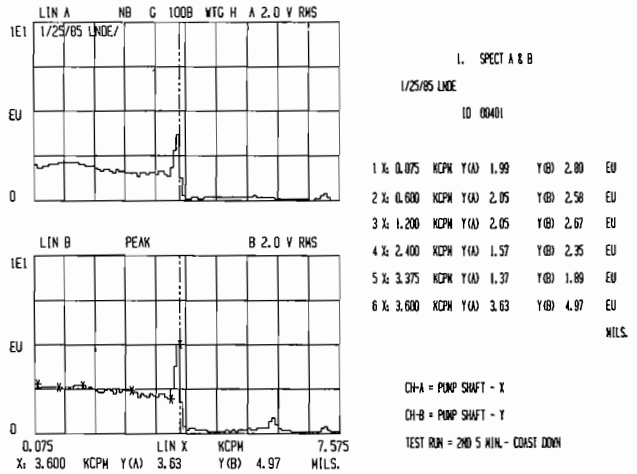

Figure 16. Pump Vibration After Implementation of Solution 1.

Table 2. Comparison of Vibration Data Before and After Design Modification.

(All vibration data are in mm (mils), peak-to-peak)

	BEFORE MODIFICATION (10/9/84)		AFTER MODIFICATION (1/25/85)		(11/6/85)	
	X-PROBE	Y-PROBE	X-PROBE	Y-PROBE	X-PROBE	Y-PROBE
TOTAL VIBRATION MEASUREMENTS	0.204 (8.03)	0.193 (7.60)	0.0922 (3.63)	0.126 (4.97)	0.117 (4.61)	0.104 (4.09)
RUNOUT (AT 150 RPM)	0.062 (2.44)	0.071 (2.79)	-----	-----	-----	-----
RUNOUT (AT 75 RPM)	-----	-----	0.051 (1.99)	0.071 (2.80)	0.053 (2.09)	-----

operation of 2500 hr between the two measurement dates indicated in Table 2.

SUMMARY AND CONCLUSIONS

A problem-solving experience related to the resolution of vibration problem of a vertical multistage cryogenic pump has been outlined. A combined experimental and analytical approach was taken to assess the nature of the problem and to define practical design modifications to resolve the problem. The pump was analytically modelled as a dual level rotor bearing system to properly take into account the vibration characteristics of the pump support structure. Care has been taken to model all parts of the pump, including wear rings, bearing bushings, throttle bushing, bottom bearing bushing, coupling, motor pedestal, and the motor. Test data were used to calibrate the analytical model, which yielded several practical solutions to the pump's vibration problem. Field data confirmed the usefulness of the implemented solution. The vibration problem of the pump was successfully resolved. The following conclusions may be drawn:

- The modelling of this vertical pump as a dual level rotor bearing system is intuitively valid and technically correct. Modelling the pump as a single level system is shown to cause an important subsynchronous mode to remain undetected, and the system's stability margin overestimated. The dual

level model used herein is properly calibrated by matching prediction for the baseline case with test data of support structure vibrations and relative shaft vibration taken at three different stations. Proper modelling of the motor pump unit to account for the vibrations of the pump support structure and pump casing bundle is as important as the use of correct models for its components and/or accurate numerical values for the pump's critical dimensions.

- The empirical models for wear rings, bearing bushings, and stator-impeller forces used in this study are obtained from current literature. Experience reported herein has been that the synchronous response predicted for the above ground stations of this pump with a long flexible shaft, does not vary sensitively with the numerical values of the dynamic coefficients of these components in the ranges studied.
- A combined analytical and experimental approach is an effective way to systematically resolve vibration problems of vertical multistage pumps of the type studied. Many empirical methods of solutions described in the literature are machine specific, not generally applicable to other pumps. On the other hand, the method of solution presented, especially the dual level modelling technique, should be applicable to all vertical pumps.

REFERENCES

1. Gunter, E. J., Lindsey, S. F., and Muschick, R. P., "Stability and Time Transient Analysis of Oconee 24-Stage High Pressure Injection Pump," Duke Power Company Report, Charlotte, North Carolina (June 1985).
2. Gopalakrishnan, S., and Usui, Y., "Critical Speed of Centrifugal Pumps," The Shock and Vibration Digest, *16*, (4), pp. 3-10 (April 1984).
3. Gopalakrishnan, S., Fehlau, R. and Lorett, J., "How to Calculate Critical Speed in Centrifugal Pumps," Oil & Gas Journal, pp 113-119 (December 7, 1981).
4. Bosmans, R.F., "Hydraulic Induced Instability on a Vertical Service Water Pump: Case History," Proceedings of Symposium on Instability in Rotating Machinery, Bently Nevada Dynamics Research Corporation, Carson City, Nevada (June 10-14, 1985).
5. Black, H. F., "Effects of Fluid Filled Clearance Spaces on Centrifugal Pump and Submerged Motor Vibrations," *Proceedings of the Eighth Turbomachinery Symposium*, Turbomachinery Laboratories, Department of Mechanical Engineering, Texas A&M University, College Station, Texas (1979).
6. Childs, D. W., "Finite Length Solutions For Rotordynamic Coefficients of Turbulent Annular Seals," Journal of Lubrication Technology, Trans. ASME, *105*, pp. 437 -445 (July 1983).
7. Allaire, P. E., Gunter, E. J., Lee, C. P. and Barrett, L. E., "The Dynamic Analysis of the Space Shuttle Main Engine High Pressure Fuel Turbopump," Final Report, Part III, Load Capacity and Hybrid Coefficients For Turbulent Interstage Seals, NASA Marshall Space Flight Center (September 1976).
8. Kim, C., and Childs, D. W., "Analysis for Rotordynamic Coefficients of Helically-Grooved Turbulent Annular Seals," ASME Journal of Tribology, *109*, pp. 136-143 (January 1987).
9. Jery, B., Acosta, A. J., Brennen, C. E., and Caughey, T. K., "Hydrodynamic Impeller Stiffness, Damping and Inertia," Proceedings of the Third Workshop on Rotordynamic Instability Problems in High-Performance Turbomachinery, College Station, Texas, NASA Conference Publication No. 2338, pp. 137-160 (1984).
10. Jery, B., Brennen, C. E., Caughey, T. K., and Acosta, A. J., "Forces on Centrifugal Pump Impellers," *Proceedings of the Second International Pump Symposium*, Texas A&M University, College Station, Texas, pp. 21-29 (April 1985).
11. Chamieh, D. S., Acosta, A. J., Brennen, C. E., Caughey, T. K., and Franz, R., "Experimental Measurements of Hydrodynamic Stiffness Matrices for a Centrifugal Pump Impeller," Proceedings of Second Workshop on Rotordynamic Instability Problems in High Performance Turbomachinery, Texas A&M University, College Station, Texas, NASA Conference Publication No. 2250, pp. 382-398 (1982).
12. Gopalakrishnan, S., "Pump Instability Phenomena Generated by Fluid Forces," Proceedings of Symposium on Instability in Rotating Machinery, Bently Nevada Dynamics Research Corporation, Carson City, Nevada (June 10-14, 1985).
13. Starr, D. E., "Trouble-Shooting Vertical Pumps Utilizing Vibration Techniques," Proceedings of Machinery Vibration Monitoring and Analysis Seminar, Vibration Institute, Clarendon Hills, Illinois, pp. 131-133 (1983).
14. Jones, R. M., "Vertical Reactor Coolant Pump Instabilities," Proceedings of Symposium on Instability in Rotating Machinery, Bently Nevada Rotordynamics Research Corporation, Carson City, Nevada (1985).
15. Makay, E., "How Close are Your Feed Pumps to Instability Caused Disaster?" Power, pp. 69-71 (December 1980).
16. Meyer, R. J., "Solve Vertical Pump Vibration Problems," Hydrocarbon Proceeding, *56*, (8), pp. 145-149 (August 1977).
17. Sosa, F. and Baker, E. W., "Reduced Casing Vibrations on Large Vertical Circulating Water Pumps," ASME Paper, No. 77-FE-28 (1977).
18. Marenco, S. G., et al., "Elastic Solution for Vibration Trouble on Vertical Pumps," Energ. Ellettr., *59*, Suppl. to No. 10 (1982), paper in Conference on Rotordynamic Problem in Power Plants, Rome, Italy, pp. 429-437 (1982).
19. Goldman, S., "Solving Pump Problem Using Vibration Spectrum Analysis," Noise Vibration Control Worldwide, *12*, (8), pp. 326-331 (November 1981).
20. Mondy, R. E., and Suesli, J., "Pump Modifications Solve Complex Vibration Problems," Power, pp. 41-43 (February 1985).
21. Mondy, R. E., "Absorber Stops Elusive Multi-Stage Pump Vibration," Power, pp. 51 - 52 (March 1985).
22. Smith, D. R., and Woodward, G. M., "Vibration Analysis of Vertical Pumps," *Proceedings of the Fifteenth Turbomachinery Symposium*, Turbomachinery Laboratory, Department of Mechanical Engineering, Texas A&M University, College Station, Texas, pp. 61-68 (1986).
23. Li, D. F. and Gunter, E. J., "Unbalance Response Analysis of Dual-Rotor Systems: A Manual for Use with the Computer Program RESP2V3," Report MAE 78/150, Department of Mechanical and Aerospace Engineering, University of Virginia, Charlottesville, Virginia (1978).

ACKNOWLEDGEMENTS

The authors acknowledge the helpful discussions with Drs. P. E. Allaire and L. E. Barrett, and Mr. Joe Knight of the University of Virginia ROMAC Industrial Consortium, concerning the modelling of bushings and the numerical accuracy of the extended RESP2V3 computer code.